Vol. 40, No. 2 (2018) 326-334, DOI: 10.24874/ti.2018.40.02.15

Tribology in Industry

www.tribology.fink.rs

RESEARCH

Tribocorrosion Behavior of Amorphous Carbon-Silicon Coated Titanium in Biological Medium

J. Bautista-Ruiz[a], J.C. Caicedo[b], W. Aperador[c]

[a]*Department of Electromechanical Engineering, Universidad Francisco de Paula Santander, San José de Cúcuta, Colombia,*
[b] *Tribology, Polymers, Powder Metallurgy and Processing of Solid Recycled Research Group, Universidad del Valle, Cali, Colombia,*
[c] *Universidad ECCI, Bogotá, Colombia.*

Keywords:

Carbon-silicon films
Wear
Corrosion
Plasma-assisted chemical vapor deposition

Corresponding author:

Jorge Bautista-Ruiz
Department of Electromechanical Engineering, Universidad Francisco de Paula Santander, Avenida Gran Colombia No. 12E-96, San José de Cúcuta, Colombia.
E-mail: g.ing.materiales@gmail.com

A B S T R A C T

Studies of materials in biomedical applications have focused on the generation of new biomaterials and the development of surface modifications, mainly of metals. Amorphous silicon containing diamond like carbon DLC-Si coating deposited on titanium substrate with the purpose of studying its biofunctionality. The behavior against the phenomenon of tribocorrosion of coatings DLC-Si deposited on titanium was evaluated, through the plasma-assisted chemical vapor deposition technique. The nanoindentation technique was used to determine the coating mechanical properties. The DLC-Si coatings were structurally analyzed through X-ray diffraction (XRD) and X-ray photoelectron spectroscopy (XPS) techniques, the characteristic binding energy for the signal C1s was obtained from XPS. Via XRD results the amorphous structure of DLC-Si coating was determined. The triboelectrochemical results indicate that the coating shows an adequate wear and to corrosion protection when exposed to the synergic mechanism, thus demonstrating the protective coating effect.

1. INTRODUCTION

The synthesis DLC (diamond like carbon) in thin layers has been reported since the beginning of the 1980s. Its studies have been numerous due to the diamond-like properties, therefore, this material presents interesting industrial applications associated to mechanical, optical and electrical properties [1-2]. However, the DLC material displays functional problems from high stress and low adhesion to substrate, which substantially restricts the industrial applications [3-4]. Many studies report the use of several metals such as Au, Cu, Ag, Cr, Ti, W and Ta to decrease the high mechanical stress. Another proposal to combine the amorphous carbon DLC films with silicon material was carried out, because this system can achieve good adhesion and good mechanical properties, such as hardness and wear resistance [5]. This type of study was related to interface between metals or ceramics and amorphous carbon films results,

therefore, the proposed studies have related to the silicon content into DLC material deposited mostly on steels substrate [6].

Stainless steel biomaterial is generally the most used biomaterial in the biomedical industry; however, it has been replaced by titanium alloys. The iron-carbon alloy (316LVM stainless steel) presents 11 % of chromium, this chromium is responsible of generating an alloy with high corrosion resistance in relation to ferrous and non-ferrous metals [7-8]. The mechanical properties and high corrosion resistance of the steel makes it suitable for use in aggressive environments as heat exchanging equipment for the oil or dairy industry, wastewater treatment and biomedical implants, amongst others, [9-10]. Despite this considerable corrosion resistance, these stainless steels are susceptible to pitting corrosion in chloride environments [11], it is for this reason that other types of metals are established as replacement for their application as biomaterials. Titanium material has been used for biomedical applications compared to stainless steel and metallic-Cobalt applications; the Young's modulus for titanium is around 110 GPa, 200 GPa for stainless steel and 220 GPa for metallic-Cobalt alloys [12-13]. Taking into account the elastic modulus of the bone (20 GPa), and moreover is understood that titanium devices within the human body are elastically supported by natural tissues, titanium has poor shear strength; in this sense, this material cannot be used in bolts and screws. To prevent complications, the new development of Ti alloys are concentrated in β alloys which are less rigid than α and α + β alloys with elastic modulus of 50 GPa.

For tribological applications many coatings on titanium implants have revealed that adhesive in the sliding regime and abrasion effects are the predominant wear mechanisms [14,15]. One alternative for improving the performance of joint replacements are hard coatings as technical applications, like cutting tools and machining, which rise substrate properties improving wear and corrosion resistance [16]. Within these coatings are diamond like carbon (DLC), which is a material with outstanding mechanical, tribological and biological properties [17].

In the present work, amorphous carbon-silicon films (DLC-Si) coatings were deposited on titanium substrates with the aim to study the tribo-chemical performance of DLC-Si coatings. Tribocorrosion tests were carried out on the coated samples by using a bone pin under Ringer´s physiological solution (electrolyte like simulated fluid); simulating biological wear conditions.

2. EXPERIMENTAL SECTION

Titanium samples were used as substrates, cut with wire cutting EDM process at 5 mm/min. After cutting they were polished with silicon carbide paper from 80 to 1200, and finally a micro cloth was used. The deposition of the diamond-like carbon (DLC) coating was carried out utilizing plasma enhanced chemical vapor deposition (PECVD) techniques. The titanium substrates were placed in a water-cooled cathode supplied by asymmetric bipolar pulsed DC source. Subsequently, vacuum was generated, then the system was purged and a second cleaning with Argon plasma was carried out for 30 minutes in order to remove any surface oxide layer. After, the chamber was put through to a high vacuum of 10^{-6} Torr. To improve the adhesion of the DLC coating, intermediate layers of fine amorphous silicon (~ 100 nm) were generated, using silane as a precursor for 15 minutes. Then, the acetylene was allowed to enter at a pressure that is in the range of 2.5 x 10^{-3} Torr; the waveform consisted of a fixed positive pulse of 30 V followed by a variable negative pulse that ranges from -250 to -700 V; a frequency of 20 kHz was used in the pulse; the films were deposited with methane at a pressure of 10 Pa to 10 sccm of flow.

XPS measurements were performed in ultrahigh vacuum with base pressure of 2×10^{-10} mbar using a Phoibos 100 ESCA/Auger spectrometer with Mg Kα anode (1253.6 eV) after a short etching of the samples' surface in order to remove contamination. To avoid X-ray damage on the samples, low X-ray power of 150 W was used.

The nanoindentation measurements were developed in a NanoTest 550 nanoindentator (Micro Materials, Ltd) that had a Berkovich type indenter, with a resolution of 1 μN and 1 nm in load and displacement, respectively. After initial tests with a coating, the following parameters were used: depth controlled experiment, to 400 nm depth; 0.02 mN/s load rate; indenter held at

maximum depth for 30 s; indenter held at 80 % unloading for 30 s. Several indentations were developed on each sample and the data averaged.

The X-ray diffraction measurements were carried out by using a Bruker D8 Advance X-ray diffractometer. The X-rays were produced using a sealed tube, the x-ray wavelength was 0.154 nm (Cu K-alpha) and were detected using a fast counting detector based on Silicon strip technology (Bruker LynxEye detector).

The tribocorrosion test was developed by using assays friction, the tribochemical wear was performed on a tribometer with linear reciprocating movement (CSEM tribometer) and geometry sphere-plate by using two surface counter pairs, pin (bone) and disk (Ti/DLC-Si coatings). The bone pin was prepared from a bovine metacarpal diaphysis, which was immersed in boiling water while avoiding touching the bottom of the vessel so as not to degrade its mechanical properties. Then the soft tissue was removed mechanically by hand and the bone was immersed in a bleach-water mixture for 75 hours, later further machined to a spherical geometry of 6 mm diameter.

To establish the duration of the test, the average distance travelled by patients undergoing hip arthroplasty was taken into account. To determine this distance it is important to establish the sliding arch in the femoral head. According to studies, on average, patients who undergo this type of intervention are elderly patients. It is estimated that during their recovery they travel about 500 m per day, with an average length of 0.35 m in each step, resulting in a total of 1429 steps per day approximately. In this research the maximum running time was associated to 140 m.

The tests were carried out in aerated Ringer physiological solution (electrolyte like simulate fluid), at 37 °C, composed of NaCl (9 g), KCl (0.4 g), $CaCl_2$ (0.17 g) and $NaHCO_3$ (2.1 g). Ringer's solution is a solution of several salts dissolved in water for the purpose of creating an isotonic solution relative to an animal's bodily fluids. Therefore, Ringer's solution typically contains sodium chloride, potassium chloride, calcium chloride and sodium bicarbonate, with the last used to balance the pH. The precise proportions of these vary from species to species, particularly between marine osmoconformers and osmoregulators. Ringer's solution is frequently used in in-vitro experiments for organs or tissues, such as in-vitro muscle testing [17].

In the tribological test a constant load of 5 N was applied with an oscillation frequency of 1 Hz. The length travelled by the sphere in each cycle was 8 mm, with the total sliding distance of each test being 500 m. The average friction coefficient and the wear coefficients of both the sphere and the coating were determined.

In order to study the influence of the synergy between abrasive wear and corrosion effect, the, tribocorrosion test was carried out by using a CSEM tribometer at a temperature of 37 ±0.2 °C (normal body temperature). The tribometer was adequate with an electrochemical cell consisting of a series of three electrodes, reference (Ag/AgCl), counter electrode (platinum wire) and work based on a specimen with an area of exposure of 1 cm^2. Autolab PGSTAT-302 (Eco Chemie) potentiostat/galvanostat with a BSTR-10A current booster was employed in all experiments using the technique of Electrochemical Impedance Spectroscopy (EIS) and Tafel polarization curves for the wear and corrosion resistance evaluation. The polarization curves were measured with a scanning rate of 1 mV/s, in range voltages from -250 mV to +250 mV with respect to corrosion potential (Ecorr). The values of corrosion current density (icorr) and corrosion potential (Ecorr) were obtained from the polarization curves by extrapolation of the cathodic an anodic slope. The Nyquist frequency diagrams were obtained between 0.001 Hz and 100 kHz by using amplitude of the sinusoidal signal by 10 mV. All electrochemical measurements were repeated at least three times to examine the reproducibility of the results.

3. RESULTS

3.1 X-Ray photoelectron spectroscopy

In Fig. 1, after of deconvolution processes, the XPS result shows the signal C1s, obtained for the amorphous carbon film with silicon content. The peak of greatest magnitude corresponds to the signal C 1s, with position 284.50 eV and width of approximately 1.9 eV; these values

coincide with other studies with the type of amorphous carbon film.

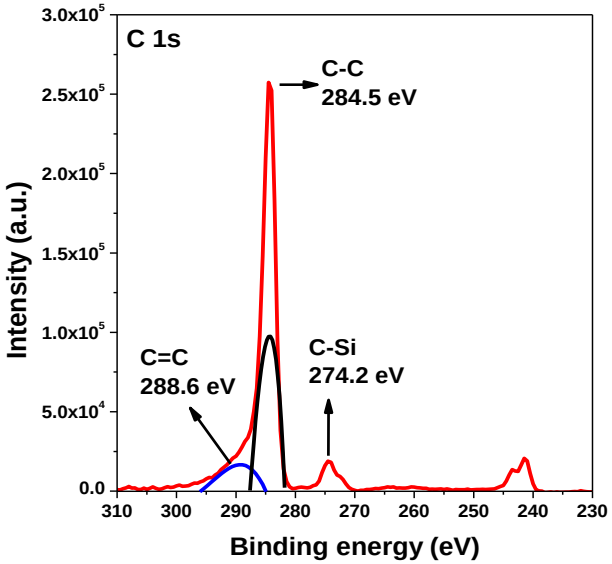

Fig. 1. XPS of the DLC film deposited on titanium, showing peaks corresponding to C1s.

The peak located at 274.25 eV corresponds to the Si-C system, this binding energy depends on the chemical environment; these values coincide with other studies with the type of amorphous carbon film. Therefore, a stoichiometric relation of $Si_{0.21}$-$C_{0.79}$ for the Si-C system was determined [5,18].

3.2 X-ray diffraction

In Fig. 2, the XRD results for the Ti substrate present the beta-Ti phase corresponding to the crystal system (Hexagonal) with a space group of P63/mmc (194).

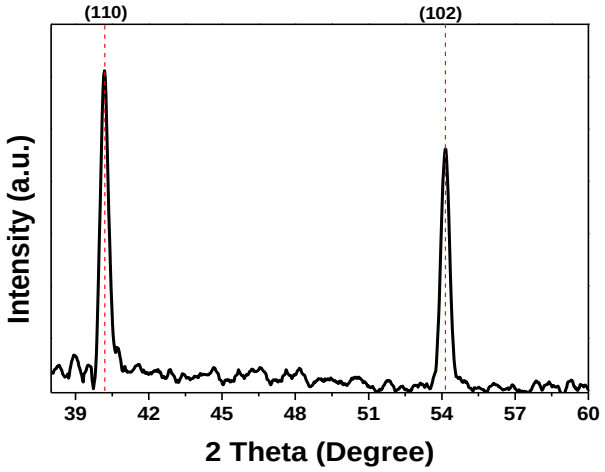

Fig. 2. X-ray diffraction spectrum, corresponding to the titanium substrate.

In the XRD pattern in analyzed tow peak associated to the Bragg direction in 2theta = 40.41° for (100) and 2theta = 53.95° for (102). These XRD results are in agreement with international JCPDF card 00-001-1198 [19].

In Fig. 3, the X-ray diffraction patterns of the DLC-Si carbon film deposited on titanium substrate are shown.

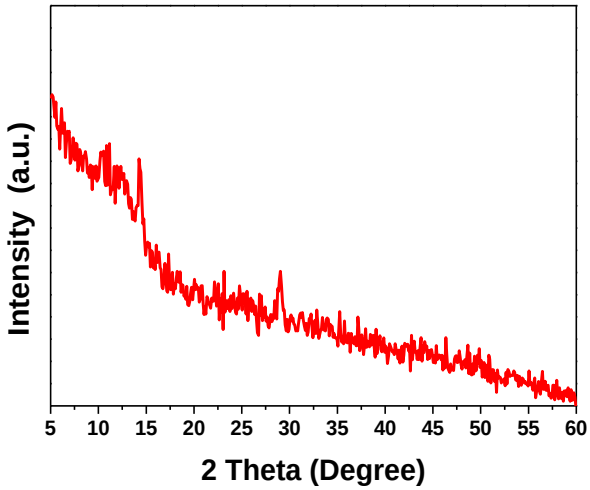

Fig. 3. X-ray diffraction pattern of DLC-Si coating, where the amorphous structure is observed.

The XRD results reveal an amorphous structure, since there are no peaks in the Bragg direction with high intensity characteristic of crystalline carbon, therefore the crystalline continuity is interrupted in the transition from crystalline carbon to DLC coating which is related to the physical and properties [20].

3.3 Hardness

Figure 4 shows the nanoindentation curve (discharge as function of indentation depth) while applying the Oliver and Pharr method. The result is the measurement of hardness (H). The indenter has a three-sided pyramid type Berkovich geometry and is generally the most accepted for the measurement of hardness in thin layers. In this way, by making several indentations and increasing the load, it is possible to represent a transition of the mechanical properties between the zones dominated by the layer [18]. From nanoindentation measurements the harness with a value of 20.2 GPa was found, so was Young's modulus with a value of 209.21 GPa. Moreover, it was possible to determinate the plastic deformation resistance of around 0.18 GPa and the elastic recovery of 61.7 %.

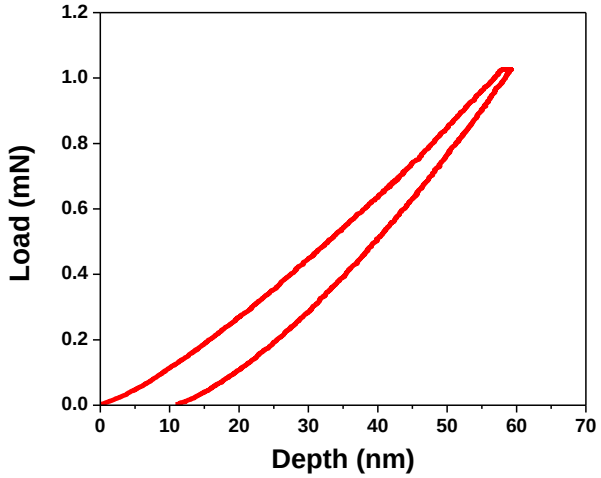

Fig. 4. Nanoindentation curve (discharge as function of indentation depth) obtained for the DLC coating.

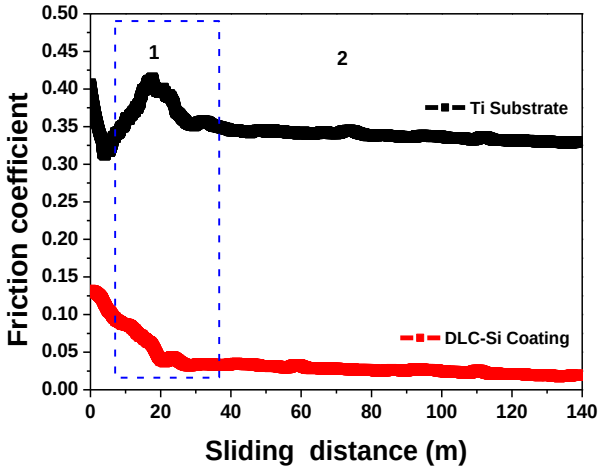

Fig. 5. Evolution of surface corrosion wear generated on the samples tested by a tribometer adapted to the electrochemical cell.

3.4 Tribocorrosion Performance

In Fig. 5, the friction coefficient as function of the sliding distance for the Ti substrate and the DlC-Si coating are observed. In the results it is possible to find two zones for all materials, zone 1 can be associated to the first zone where both surfaces (pin and coating or substrate) have a high interaction (highest friction). For the Ti substrate it is possible to observe the highest friction coefficient (0.42) for zone 1 considered starting friction during the first 20 meters in the sliding distance, the high friction coefficient is due to titanium's roughness [20]. For DLC-Si coating deposited on Ti substrate a low friction coefficient of around 0.02 was found. In zone 1 the adhesion between the surface asperities and relative movement between two surfaces can generate fracturing of the adhered films generating worn particles (debris) [21]. After this first region zone 1, Fig. 5, shows a reduction in the friction coefficient, due to a settlement distance which is produced by the difference in the surface roughness (zone 2). In zone 2 the reduction in the initial surface roughness can be related with friction coefficient reduction. In last region, the coefficient of friction stabilizes at 0.33 for the Ti-substrate material and 0.002 for DLC-Si coating. These changes are associated with the corrosion and wear phenomena. The observed phenomenon (low friction coefficient) after first region (zone 1) can be attributed to reduction of surface degradation generated by the materials' interactions; however both mechanisms such as wear and corrosion can produce more asperities, increasing the surface roughness and friction coefficient [22].

For DLC coating the friction coefficient is reduced in relation to the Ti-Substrate due to the high hardness and elastic modulus; Moreover, the covalent bound present in the C-Si system offers high corrosion resistance [23]. Therefore, the high elastic modulus and high corrosion resistance generate high wear resistance to the synergism between high friction and electrochemical effect. Comparing two systems, titanium and DLC-Si, a better behavior of coated samples is seen based on the difference that is perceived in the surfaces. It can be inferred that with greater variation in topography, greater degradation occurs either by the mechanism of wear or by corrosive effect [24].

3.5 Electrochemical Impedance Spectroscopy (EIS)

In Fig. 6, the Nyquist diagram was carried out after the stabilization of corrosion potential during the test. After, the electrochemical responses of titanium substrate and the DLC-Si coating were compared. The curve generated indicates the adequate performance achieved by the coating since it increases the total impedance of system by more than two times. This is due to effect of protective DLC-Si coating, whose porosity and roughness are in nanometers, which generates a decrease in the frequency dispersion [25]. The structure obtained generates an excellent behavior as a consequence of the interface that exists between the substrate and the DLC layer, generated by silicon, which allows a smooth transition system rather than between the configurations of two systems.

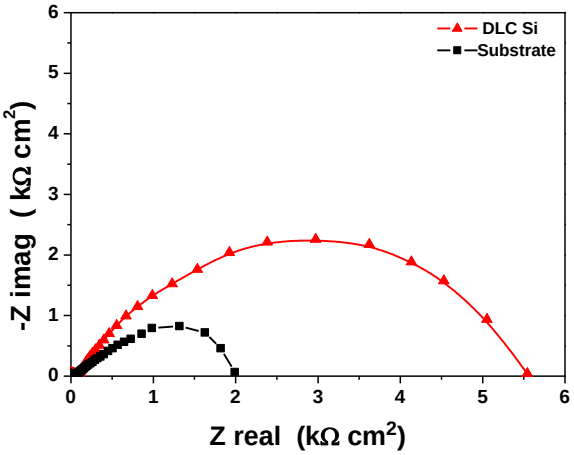

Fig. 6. Impedance of DLC-Si coating and uncoated titanium substrate, in corrosion wear system with ringer lactate solution.

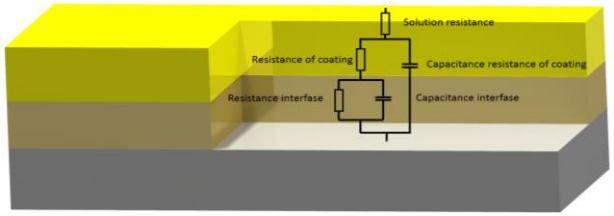

Fig 7. Equivalent electrical circuit modeled from EIS results. The result is modeled with variables obtained from the chemical-mechanical interaction of the coating, substrate and electrolyte (simulate fluid).

The total thickness of the DLC-Si coating was around 2 µm. Taking into account the coating thickness, the binding lining layer in the coating was analyzed as a single element, so that an alternating current scheme is corresponding to the equivalent circuit where there is a resistance to polarization that indicates the protective layer effect in parallel with a constant phase element, evidencing the adequate adherence of the coating to titanium substrate (Fig. 7) [26].

3.6 Potentiodynamic curves

Figure 8 shows the potentiodynamic curves corresponding to titanium substrate and DLC-Si coating. Ti substrate displayed a corrosion potential close to anodic zone, which generates an adequate electrochemical performance. The anodic region indicates a passivation zone, because the corrosion current decreases when the potential increases, in agreement with increase in the corrosion rate [27]. The last behaviour is due to oxide layer formed spontaneously, which is very thin and can be attacked by the chlorides contained in Ringer´s solution [28-29]. From Tafel results it is possible to observe that DLC coating presents a better corrosion performance, because the corrosion current density in relation to titanium substrate shifts towards lower current values, which generates a chemical inertia and increases the corrosion resistance. The potentiodynamic curve for DLC-Si coating exhibits a decrease in corrosion current in the anodic zone, much less than that observed by titanium, indicating the coating passivation [30].

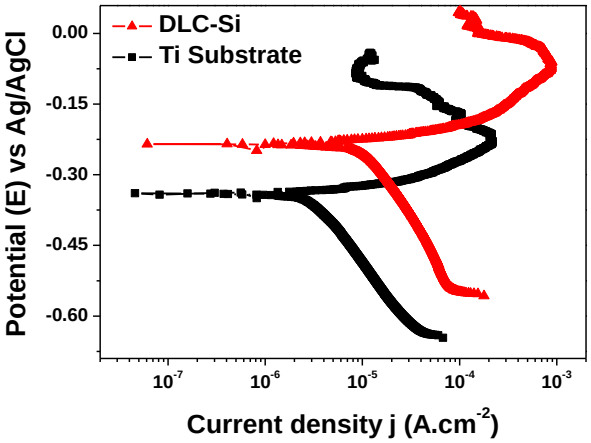

Fig. 8. Potentiodynamic polarisation curves (Tafel) of uncoated titanium substrate and DLC- Si coating.

Table 1. Corrosion rate results for Ti substrate and the DLC - Si coating.

	Corrosion potential / mV	Corrosion current density / µA-cm^{-2}	Corrosion rate / mpy
Titanium	-781	11.41	5.18
DLC - Si	-1134	3.91	1.77

Table 1 shows the values obtained from the polarization curve. The Ti substrate and coating results were compared, determining that the DLC-Si coating represents a low value of corrosion current and corrosion rate, corroborating the decreasing degradation effect.

3.7 SEM Results

Figure 9 shows the SEM micrograph before the tribo-corrosion test, where it is possible to observe that the DLC-Si coating deposited on the Ti substrate presents a high homogeneity without any surface delamination generated by cracks, pitting and wear damage.

Figure 10 presents the SEM micrograph of DLC-Si coating deposited on Ti substrate after tribo-corrosion test.

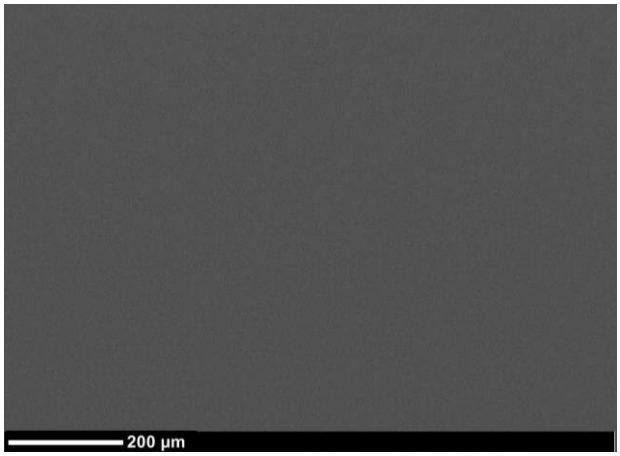

Fig. 9. SEM micrograph of DLC-Si coating deposited on Ti substrate, before tribo-corrosion test.

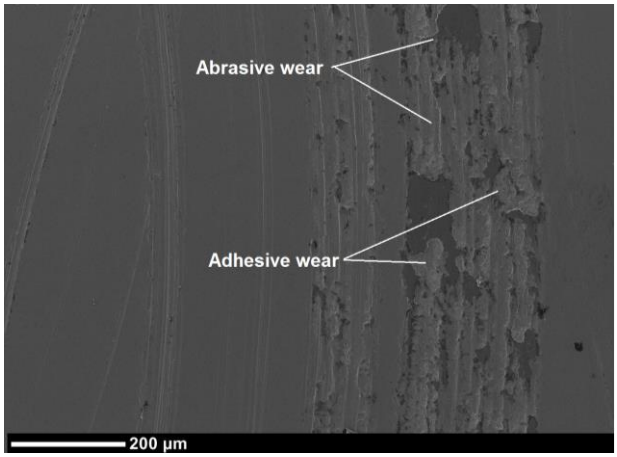

Fig. 10. SEM micrograph of DLC-Si coating deposited on Ti substrate after tribo-corrosion test.

It is possible to observe the wear track which shows different wear mechanisms, such as adhesive wear and abrasive wear. Taking into account the last discussion, the wear mechanism can be related to the tribology system formed by the DLC-SI coating surface and the pin surface under the Ringer´s physiological solution. Therefore, the adhesive wear can be formed from transferred bone films on the DLC-Ti coating surface during the sliding distance that was carried out [31-33].

4. CONCLUSIONS

The electrochemical wear evaluation of the titanium substrate coated with DLC-Si material shows a surface degradation process when exposed to wear-corrosion effect, which is represented for the material loss and the heterogeneity generation on the DLC-Si surface, thus increasing the surface roughness. Therefore, it can be inferred that high surface roughness produces corrosive and wear processes. In this sense, the DLC-Si coating protects the system by eliminating surface ridges.

With electrochemical measurements an adequate coating protection was observed, equivalent to two times in relation to total impedance of system and can be analyzed a decreasing of three times of degradation rate. So, this behavior is due to the interface that exists between the Ti substrate and the DLC-Si coating, which allows a smooth transition between the union of the two surfaces (Ti and DLC-Si). The polarization resistance value of the coating indicates a protective effect generated by the system due to low friction coefficient and high corrosion resistance.

Author Contributions: Willian Aperador performed the obtaining coatings; Jorge Bautista worked in measurements in SEM, AFM and XRD and performed the interpretation of the data and the respective analysis. Julio Caicedo performed measurements corrosion tests performed the interpretation of the data.

REFERENCES

[1] T. Laurila, S. Sainio, M.A. Caro, *Hybrid carbon based nanomaterials for electrochemical detection of biomolecules*, Progress in Materials Science, vol. 88, pp. 499-594, 2017, doi.org/10.1016/j.pmatsci.2017.04.012

[2] S. Muhl, A. Pérez, *The use of hollow cathodes in deposition processes: A critical review*, Thin Solid Films, vol. 579, pp. 174-198, 2015, doi.org/10.1016/j.tsf.2015.02.066

[3] A. Doi, H. Kawai, T. Yoshioka, S. Yamanaka, *Vapor-deposited ceramic coating: Status and prospects*, Ceramics International, vol. 18, iss. 4, pp. 223-229, 1992, doi.org/10.1016/0272-8842(92)90099-Y

[4] R. Franz, C. Mitterer, *Vanadium containing self-adaptive low-friction hard coatings for high-temperature applications: A review*, Surface and Coatings Technology, vol. 228, pp. 1-13, 2013, doi.org/10.1016/j.surfcoat.2013.04.034

[5] R. Kr. Ghadai, S. Das, D. Kumar, S. C. Mondal, B.P. Swain, *Correlation between structural and mechanical properties of silicon doped DLC thin films*, Diamond and Related Materials, vol. 82, pp. 25-32, , 2018, doi.org/10.1016/j.diamond.2017.12.012

[6] Md Abdullah Al Mamun, H. Furuta, A. Hatta, *Pulsed DC plasma CVD system for the deposition of DLC films*, Materials Today Communications, vol. 14, pp. 40-46, 2018, doi.org/10.1016/j.mtcomm.2017.12.008

[7] R.A. Antunes, M.C. Lopes de Oliveira, *Corrosion fatigue of biomedical metallic alloys: Mechanisms and mitigation*, Acta Biomaterialia, vol. 8, iss. 3, pp. 937-962, 2012, doi.org/10.1016/j.actbio.2011.09.012

[8] J.J. Ramsden, D.M. Allen, D.J. Stephenson, J.R. Alcock, G.N. Peggs, G. Fuller, G. Goch, *The Design and Manufacture of Biomedical Surfaces*, CIRP Annals, vol. 56, iss. 2, pp. 687-711, 2007, doi.org/10.1016/j.cirp.2007.10.001

[9] S. Cui, S. Lu, W. Xu, B. An, B. Wu, *Fabrication of robust gold superhydrophobic surface on iron substrate with properties of corrosion resistance, self-cleaning and mechanical durability*, Journal of Alloys and Compounds, vol. 728, pp. 271-281, 2017, doi.org/10.1016/j.jallcom.2017.09.007

[10] J. Zuo, Y. Xie, J. Zhang, Q. Wei, B. Zhou, J. Luo, Y. Wang, Z.M. Yu, Z.G. Tang, *TiN coated stainless steel bracket: Tribological, corrosion resistance, biocompatibility and mechanical performance*, Surface and Coatings Technology, vol. 277, pp. 227-233, 2015, doi.org/10.1016/j.surfcoat.2015.07.009

[11] J. Verma, R. V. Taiwade, *Effect of welding processes and conditions on the microstructure, mechanical properties and corrosion resistance of duplex stainless steel weldments—A review*, Journal of Manufacturing Processes, vol. 25, pp. 134-152, 2017, doi.org/10.1016/j.jmapro.2016.11.003

[12] M.F.F.A. Hamidi, W.S.W. Harun, M. Samykano, S.A.C. Ghani, Z. Ghazalli, F. Ahmad, A.B. Sulong, *A review of biocompatible metal injection moulding process parameters for biomedical applications*, Materials Science and Engineering: C, vol. 78, pp. 1263-1276, 2017, doi.org/10.1016/j.msec.2017.05.016

[13] M. Niinomi, M. Nakai, J. Hieda, *Development of new metallic alloys for biomedical applications*, Acta Biomaterialia, vol. 8, iss. 11, pp. 3888-3903, 2012, doi.org/10.1016/j.actbio.2012.06.037

[14] M.T. Mohammed, *Development of a new metastable beta titanium alloy for biomedical applications*, Karbala International Journal of Modern Science, vol. 3, iss. 4, pp. 224-230, 2017, doi.org/10.1016/j.kijoms.2017.08.005

[15] Y. Li, K. S. Munir, J. Lin, C. Wen, *Titanium-niobium pentoxide composites for biomedical applications*, Bioactive Materials, vol. 1, iss. 2, pp. 127-131, 2016, doi.org/10.1016/j.bioactmat.2016.10.001

[16] E.D. Gonzalez, Conrado R.M. Afonso, Pedro A.P. Nascente, *Influence of Nb content on the structure, morphology, nanostructure, and properties of titanium-niobium magnetron sputter deposited coatings for biomedical applications*, Surface and Coatings Technology, vol. 326, part B, pp. 424-428, 2017, doi.org/10.1016/j.surfcoat.2017.03.015

[17] K.H. Woll, M.D. Leibowitz, B. Neumcke, B. Hille, *A high-conductance anion channel in adult amphibian skeletal muscle*, Pflugers Archiv, vol. 410, no. 6, pp. 632–640, 1987.

[18] M. Constantinou, M. Pervolaraki, L. Koutsokeras, C. Prouskas, P. Patsalas, P. Kelires, J. Giapintzakis, G. Constantinides, *Enhancing the nanoscratch resistance of pulsed laser deposited DLC films through molybdenum-doping*, Surface and Coatings Technology, vol. 330, pp. 185-195, 2017, doi.org/10.1016/j.surfcoat.2017.09.048

[19] V. Gopal, M. Chandran, M.S. Ramachandra Rao, S. Mischler, S. Cao, G. Manivasagam, *Tribocorrosion and electrochemical behaviour of nanocrystalline diamond coated Ti based alloys for orthopaedic application*, Tribology International, vol. 106, pp. 88-100, 2017, doi.org/10.1016/j.triboint.2016.10.040

[20] R. Bayón, A. Igartua, J.J. González, U. Ruiz de Gopegui, *Influence of the carbon content on the corrosion and tribocorrosion performance of Ti-DLC coatings for biomedical alloys*, Tribology International, vol. 88, pp. 115-125, 2015, doi.org/10.1016/j.triboint.2015.03.007

[21] Z. Doni, A.C. Alves, F. Toptan, J.R. Gomes, A. Ramalho, M. Buciumeanu, L. Palaghian, F.S. Silva, *Dry sliding and tribocorrosion behaviour of hot pressed CoCrMo biomedical alloy as compared with the cast CoCrMo and Ti6Al4V alloys*, Materials & Design, vol. 52, pp. 47-57, 2013, doi.org/10.1016/j.matdes.2013.05.032

[22] K. Sadiq, M.M. Stack, R.A. Black, *Wear mapping of CoCrMo alloy in simulated bio-tribocorrosion conditions of a hip prosthesis bearing in calf serum solution*, Materials Science and Engineering: C, vol. 49, pp. 452-462, 2015, doi.org/10.1016/j.msec.2015.01.004

[23] V. Sáenz de Viteri, G. Barandika, R. Bayón, X. Fernández, I. Ciarsolo, A. Igartua, R. Pérez - Tanoira, J. Moreno, C. Pérez, J. Peremarch, *Development of Ti–C–N coatings with improved tribological behavior and antibacterial properties*, Journal of the Mechanical Behavior of Biomedical Materials, vol. 55, pp. 75-86, 2016, doi.org/10.1016/j.jmbbm.2015.10.020

[24] Y. Yan, A. Neville, D. Dowson, S. Williams, *Tribocorrosion in implants—assessing high carbon and low carbon Co–Cr–Mo alloys by in situ electrochemical measurements*, Tribology International, vol. 39, iss. 12, pp. 1509-1517, 2006, doi.org/10.1016/j.triboint.2006.01.016

[25] X. Guan, Y. Wang, J. Wang, Q. Xue, *Adaptive capacities of chromium doped graphite-like carbon films in aggressive solutions with variable pH*, Tribology International, vol. 96, pp. 307-316, 2016, doi.org/10.1016/j.triboint.2015.12.048

[26] S. Maniscalco, M. Caligari Conti, J. Cassar, C. Grima, A. Karl, P. S. Wismayer, B. Mallia, J. Buhagiar, *Low temperature carburised austenitic stainless steel for metal-on-metal tribological contact*, Thin Solid Films, vol. 620, pp. 103-113, 2016, doi.org/10.1016/j.tsf.2016.07.084

[27] Y. Wang, Y. Yan, Y. Su, L. Qiao, *Release of metal ions from nano CoCrMo wear debris generated from tribo-corrosion processes in artificial hip implants*, Journal of the Mechanical Behavior of Biomedical Materials, vol. 68, pp. 124-133, 2017, doi: 10.1016/j.jmbbm.2017.01.041

[28] C.F. Almeida Alves, F. Oliveira, I. Carvalho, A.P. Piedade, S. Carvalho, *Influence of albumin on the tribological behavior of Ag–Ti (C, N) thin films for orthopedic implants*, Materials Science and Engineering: C, vol. 34, pp. 22-28, 2014, doi.org/10.1016/j.msec.2013.09.031

[29] L.D. Trino, L.F.G. Dias, L.G.S. Albano, E.S. Bronze-Uhle, E.C. Rangel, C.F.O. Graeff, P.N. Lisboa-Filho, *Zinc oxide surface functionalization and related effects on corrosion resistance of titanium implants*, Ceramics International, vol. 44, iss. 4, pp. 4000-4008, 2018, doi.org/10.1016/j.ceramint.2017.11.195

[30] B.J. Wu, Q.Y. Deng, Y.X. Leng, C.M. Wang, N. Huang, *Characterization of adsorption and lubrication of synovial fluid proteins and HA on DLC joint bearings surface*, Surface and Coatings Technology, vol. 320, pp. 320-332, 2017, doi.org/10.1016/j.surfcoat.2016.12.058

[31] D. Choudhury, J. Lackner, R.A. Fleming, J. Goss, J. Chen, M. Zou, *Diamond-like carbon coatings with zirconium-containing interlayers for orthopedic implants*, Journal of the Mechanical Behavior of Biomedical Materials, vol. 68, pp. 51-61, 2017, doi.org/10.1016/j.jmbbm.2017.01.023

[32] K. Oguri, T. Arai, *Tribological properties and characterization of diamond-like carbon coatings with silicon prepared by plasma-assisted chemical vapour deposition*, Surface and Coatings Technology, vol. 47, iss. 1-3, pp. 710-721, 1991, doi.org/10.1016/0257-8972(91)90344-V

[33] M. Alaluf, J. Appelbaum, L. Klibanov, D. Brinkerb, D. Scheiman, N. Croitoru, *Amorphous diamond-like carbon films-a hard anti-reflecting coating for silicon solar cells*, Thin Solid Films, vol. 256, iss. 1-2, 1995, doi.org/10.1016/0040-6090(95)80024-7